Effects of 4F-phenyl pyrazole, a [6]-shogaol derivative, on colorectal adenocarcinoma cell death

Lalida Sirianant[a,*], **Podchanart Wanitchakool**[b], **Pakit Kumboonma**[c], **Nutnaree Srisarakorn**[b],
Premyuda Hempoom[b], **Chatchai Muanprasart**[d]

[a] Department of Applied Biology, Faculty of Science and Liberal Arts, Rajamangala University of Technology Isan,
    Nakhon Ratchasima 30000 Thailand
[b] Department of Clinical Microscopy, Faculty of Medical Technology, Mahidol University,
    Nakhon Pathom 73170 Thailand
[c] Department of Applied Chemistry, Faculty of Science and Liberal Arts, Rajamangala University of Technology Isan,
    Nakhon Ratchasima 30000 Thailand
[d] Chakri Naruebodindra Medical Institute, Faculty of Medicine Ramathibodi Hospital, Mahidol University,
    Samut Prakan 10540 Thailand

*Corresponding author, e-mail: lalida.si@rmuti.ac.th

ABSTRACT: Colorectal cancer remains a leading cause of cancer-related mortality globally. Apoptosis induction is a crucial target for developing effective chemotherapeutics. [6]-shogaol, a ginger-derived compound, has demonstrated anticancer potential by triggering apoptosis in various cancer types. This study investigated the apoptosis- and autophagy-inducing and antiproliferative effects of 4F-phenyl pyrazole, a synthetic [6]-shogaol derivative, in colorectal adenocarcinoma cells. Our findings demonstrated that 4F-phenyl pyrazole effectively reduced colorectal adenocarcinoma HT29 cell viability, showing comparable efficacy to [6]-shogaol with an IC_{50} of 9.7 µM. It also significantly inhibited colony formation, indicating its antiproliferative properties. Mechanistic studies revealed dose-dependent increases in phosphatidylserine exposure and anoctamin6 (ANO6) expression at 10, 20, and 40 µM after 72 h of 4F-phenyl pyrazole treatment, suggesting apoptosis induction. Similar dose-dependent effects were observed for LC3 expression, a marker of autophagy. Furthermore, 40 µM 4F-phenyl pyrazole treatment resulted in diminished spheroid formation. These results suggest that 4F-phenyl pyrazole is a promising candidate for further development as an anticancer agent. Further investigations into its therapeutic potential and underlying mechanisms are warranted.

KEYWORDS: 4F-phenyl pyrazole, apoptosis, anoctamin6, autophagy, colorectal cancer

INTRODUCTION

Colorectal cancer ranks as the third most common cancer worldwide, resulting in over 900,000 deaths in 2020 [1]. The disease often presents with symptoms such as abdominal pain, anemia, or rectal bleeding only at advanced stages, when tumors have become aggressive and metastatic. Recent years have seen an alarming increase in colorectal cancer incidence among individuals younger than 50 years old. Risk factors for colorectal cancer include genetic predisposition and lifestyle choices, such as insufficient physical activity, poor diet, obesity, smoking, and excessive alcohol consumption [2]. The pathogenesis of colorectal cancer typically involves the accumulation of irreversible DNA damage in cells located at the base of colonic crypts. These altered cells can acquire properties of cancer stem cells, leading to polyp formation and eventual progression to colorectal cancer [3].

Cancer cells are characterized by their ability to evade growth suppression and resist cell death. Defects in apoptotic pathways are key factors enabling cancer cell proliferation. Consequently, triggering apoptosis is a primary aim of many chemotherapeutic drugs [4]. Apoptosis is divided into 2 pathways, extrinsic and intrinsic. While the intrinsic pathway involves mitochondrial membrane permeabilization, the extrinsic pathway is initiated by death receptor activation. Despite these distinctions, both pathways converge on the activation of caspase-3, a key executioner enzyme in apoptosis [5]. Caspase-3 activation leads to DNA fragmentation and, ultimately, cell death. In addition to caspase-3, anoctamin 6 (ANO6), a member of the TMEM16 or anoctamin protein family, plays a crucial role in apoptosis. ANO6 functions as a Ca^{2+}-dependent phospholipid scramblase [6], facilitating the trans-bilayer transport of phosphatidylserine (PS) during apoptosis [7]. The exposure of PS to the cell surface serves as an "eat me" signal, promoting the removal of apoptotic cells by macrophages. Besides apoptosis, autophagy represents another form of programmed cell death targeted by chemotherapeutic drugs, including FOLFOX regimens [8]. Autophagy is a cellular self-degradation process characterized by the formation of phagophores and the activity of lysosomal enzymes. A key protein in this process is the microtubule-associated protein light chain 3 (LC3), which plays a crucial role in phagophore elongation and autophagosome formation. The fusion of autophagosomes with lysosomes leads to the degradation

of cellular components through the action of lysosomal enzymes. These events collectively drive the cell's self-clearance activity [9, 10].

[6]-Shogaol, a bioactive compound derived from ginger (*Zingiber officinale*), has demonstrated potent anti-cancer properties in various cancer types, including breast, prostate, lung, and colorectal cancers. This compound has been shown to induce cell cycle arrest and promote cell death through both autophagy and apoptosis [11–14]. However, the effects of [6]-shogaol derivatives on cancer cell death are not well established. Therefore, the present study aimed to investigate the potential of novel [6]-shogaol derivatives, synthesized through reaction with phenylhydrazines in ethanol at 80 °C, to induce apoptosis in colorectal cancer cells and elucidate the underlying mechanisms.

MATERIALS AND METHODS

Pyrazole derivatives of [6]-shogaol synthesis

Pyrazole derivatives of [6]-shogaol was synthesized as previously described in [15]. In brief, a solution of [6]-shogaol in ethanal and phenylhydrazine were mixed and reflux at 80 °C. The phenylhydrazines used in these experiments were phenylhydrazine hydrochloride, 0-tolylphenylhydrazine hydrochloride, 2-methoxyphenylhydrazine hydrochloride, 4-methoxy phenylhydrazine hydrochloride, 2-fluorophenylhydra zine hydrochloride, 4-fluorophenylhydrazine hydro chloride, 3-chlorophenylhydrazine hydrochloride, 4-chlorophenylhydrazine hydrochloride, 3-nitrophenyl hydrazine hydrochloride, 4-nitrophenylhydrazine hydrochloride, and 4-hydrazinobenzoicacid. The residues of the mixture after filtration were washed with ethanol and dried with anhydrous sodium sulfate, giving crude extract. The extract was then purified by column chromatography.

Cell culture

Colorectal cancer Caco2 (cat. no. HTB-37) was purchased from the American Type Culture Collection (ATCC, Manassas, VA, USA). HT29 and T84 cells were kindly provided by Prof. Dr. Chatchai Muanprasart. Cells were cultured in Dulbecco's Modified Eagle Medium (DMEM) supplemented with 10% (v/v) fetal bovine serum (Gibco, USA) and 1% (v/v) penicillin/streptomycin (Gibco). Cells were grown under standard condition, which is a humidified atmosphere incubator with 5% CO_2 and 95% air at 37 °C. Cells were subcultured when reaching 70–80% confluent, and cultured medium was replaced with fresh medium approximately 2–3 times a week.

Cytotoxicity assay

The cytotoxic effect of Pyrazole derivatives of [6]-shogaol was carried out by MTT assay. It is based on the ability of mitochondria reductase in living cells to convert MTT into formazan crystals. HT29 Caco2 and T84 cells were seeded in 96 well plate at a density of 10^4 cells/well in 5% FBS DMEM medium and were subjected to Pyrazole derivatives of [6]-shogaol 5a-5k at a concentration of 10 μM for 48 h. Subsequently, cells were washed with 1xPBS; then, 0.5mg/ml of MTT was added into each well and further incubated under standard condition for 4 h. The formazan crystals formed by living cells were then dissolved with DMSO, and the absorbance was measured by a microplate reader (Multiskan SkyHigh Microplate Spectrophotometer, Thermo Fisher Scientific, USA). The experiment was done in 4 replicates and repeated on three separate occasions. The same procedure was carried out to identify the IC_{50} of 4F-phenyl pyrazole. However, to obtain IC_{50}, a range of concentrations of 4F-phenyl pyrazole (0.001, 0.01, 0.1, 1, 2.5, 5, 10, 20, 40, 60, 80, and, 100 μM) were introduced to HT29 caco2 and T84 cells for 48 h.

Cell proliferation analysis

To investigate the effects of Pyrazole derivatives of [6]-shogaol on cell proliferation, the colony formation assay was performed. This method relies on the ability of cells to proliferate and grow into colonies. In this experiment, HT29 cells were seeded into 24-well plate at a density of 5×10^3 cells/well in 5% FBS DMEM medium with 1, 5, 10, 25, and 50 μM of 4F-phenyl pyrazole. Cells were grown under standard condition for 3 and 7 days. Then, cells were washed twice with 1xPBS and fixed with 4% paraformaldehyde for 15 min at room temperature. Following fixation, cells were stained with 0.1% crystal violet for 20 min. Excess crystal violet was removed using dH_2O. The stained cells were dried, and stained colonies of more than 50 cells were counted using image J software.

Apoptotic cells analysis

An annexin V-FITC/7-AAD double staining was used to elucidate the apoptotic cells. Annexin V-FITC efficiently binds to phosphatidylserine (PS) which is exposed during apoptosis. 7-AAD is a nonpermeable fluorescence dye which can stain DNA of death cells. In brief, HT29 cells (3×10^5 cells/well) were treated with 10, 20, and 40 μM of 4F-phenyl pyrazole in 5% FBS DMEM medium for 72 h. Then, cells were washed twice with PBS, collected, and stained with annexin V-FITC/7-AAD in annexin V binding buffer for 15 min. Subsequently, the stained cells were analyzed by flow cytometry (BD FACSCanto™ II, USA) for apoptotic cells.

Western blot analysis

To observe the effects of 4F-phenyl pyrazole on proteins involving cell death expression, Western blot analysis was performed. In this experiment HT29 cells were seeded at density of 3×10^5 cells/ml in 5% FBS DMEM

medium and treated with 10, 20, and 40 µM of 4F-phenyl pyrazole for 48 and 72 h. Thereafter, cells were collected, and protein were isolated using lysis buffer (25 mM Tris-HCl pH 7.4, 150 mM NaCl, 1 mM EDTA, 1% NP-40, and 5% glycerol). Proteins were then separated by 10% and 12.5% SDS-PAGE and transferred to a PVDF membrane (Thermo Fisher Scientific). Then, membranes were incubated with primary antibodies, including rabbit anti-ANO6 (Invitrogen, USA; 1:1000), rabbit anti-LC3B (Cell signaling, USA; 1:500), and mouse anti-actin (Invitrogen; 1:2000), overnight at 4 °C, and followed by incubation with HRP-conjugated goat anti-rabbit IgG (Invitrogen; 1:10,000) or HRP-conjugated goat anti-mouse secondary antibody (Invitrogen; 1:5,000). Subsequently, proteins were visualized using ECL detection. The immunoreactive intensity were quantify by the ChemiDoc™ MP Imaging System (Bio-Rad, USA).

Spheroid formation and analysis

To investigate the effects of 4F-phenyl pyrazole on spheroid formation, a 96-well ultra-low attachment (ULA) spheroid microplate (Corning, NY, USA) was used. HT29 cells were suspended in complete DMEM medium at the concentration of 1×10^5 cells/ml. Cells were seeded (50 µl/well) into ULA microplate and incubated for 3 days. After this, spheroids were treated with 20 ($2 \times IC_{50}$) and 40 ($4 \times IC_{50}$) µM of 4F-phenyl pyrazole for 24–48 h. Subsequently, spheroids were observed under a light inverted microscope (CKX53 Olympus, USA). All images were captured to measure projected area and solidity of HT29 spheroids using image J software. The projected area and solidity of 4F-phenyl pyrazole-treated spheroids were normalized with the projected area and solidity of vehicle control (DMSO-treated) spheroids. Then, the result was expressed as a fold change of the projected area and solidity, respectively. Both vehicle control (DMSO-treated) and 4F-phenyl pyrazole-treated groups had 6–12 replicates.

Statistical analysis

Statistical analysis was performed using one-way ANOVA followed by Dunnett's post-hoc test to compare each treatment group with the control. Data were presented as mean from at least 3 separate experiments ± SEM. A p-value < 0.05 was considered statistically significant.

RESULTS

Synthesis of Pyrazole derivatives of [6]-shogaol

In this study, [6]-shogaol was isolated from ginger as described by Kumboonma et al [16]. Pyrazole derivatives of [6]-shogaol was synthesized by the reaction of [6]-shogaol and phenylhydrazines in ethanol at 80 °C as previously described. 11 compounds (5a-5k) were

obtained from the reaction. The structures of [6]-shogaol and the 11 compounds were shown in Fig. 1.

Effects of [6]-shogaol and its derivatives on colorectal cancer cell viability

It has been shown that [6]-Shogaol exhibits the anti-cancer effects by triggering apoptosis as well as disturbing autophagy process [11, 13, 17]. Based on this finding, we investigated the effects of 10 µM pyrazole derivatives of [6]-shogaol on viability of colorectal adenocarcinoma HT-29 cells. We found that the 5f derivative, or 4F-phenyl pyrazole, which synthesized by the reaction of [6]-shogaol and 4-fluorophenylhydrazine, showed a similar degree of strong cytotoxic effect to [6]-shogaol (Fig. 2A). Therefore, 4F-phenyl pyrazole could be a promising derivative compound with anti-cancer effects and be further investigated. We further used 3 different types of colorectal adenocarcinoma cells to evaluate the anticancer effects of 4F-phenyl pyrazole. The results showed that after 48 h of treatment, 4F-phenyl pyrazole exhibited anticancer effects on 3 different cell types with different degrees as shown in Fig. 2B. A strong effect was found in HT-29 cells with the IC_{50} of 9.7 µM, followed by Caco2 with the IC_{50} of 28.7 µM and T84 with the IC_{50} of 40.1 µM. Additionally, under the same conditions, the IC_{50} of [6]-shogaol in HT29 cells was 9.5 µM (data not shown), which was very similar to that of 4F-phenyl pyrazole. From these results we decided to use HT-29 for the following experiments to further investigate anticancer effects of 4F-phenyl pyrazole.

Effects of 4F-phenyl pyrazole on cell proliferation

Apart from cell viability, effects of 4F-phenyl pyrazole on cell proliferation were also investigated. In this experiment, colony formation assay was performed in both cells treated with or without 4F-phenyl pyrazole. We found that colony formation in HT-29 cells was reduced in a dose-dependent manner when treated with 4F-phenyl pyrazole at concentrations ranging from 1 to 25 µM for 7 days, as shown in Fig. 3. The results were also observed in T84 and Caco2 cells. Similar results were observed at day 3 of treatment (data not shown). As the colony formation assay relies on the ability of a single cell to proliferate and form colonies; hence, we concluded that the decrease of colony formation observed in HT-29, T84, and Caco2 cells was due to anti-proliferative effects of 4F-phenyl pyrazole.

4F-phenyl pyrazole induces apoptosis in colorectal adenocarcinoma cells

It was reported that [6]-shogaol can induce cells into apoptosis after 24 hours of treatment [11]. 4F-phenyl pyrazole is a pyrazole derivative of [6]-shogaol and displayed cytotoxic effects on HT-29 cells; therefore, we further investigated whether the effects was
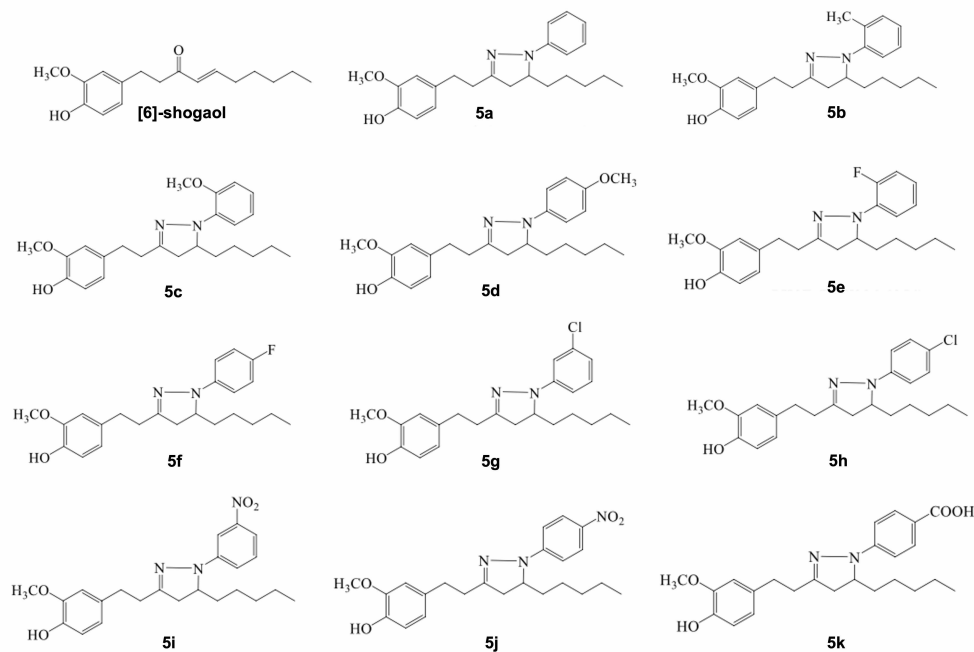
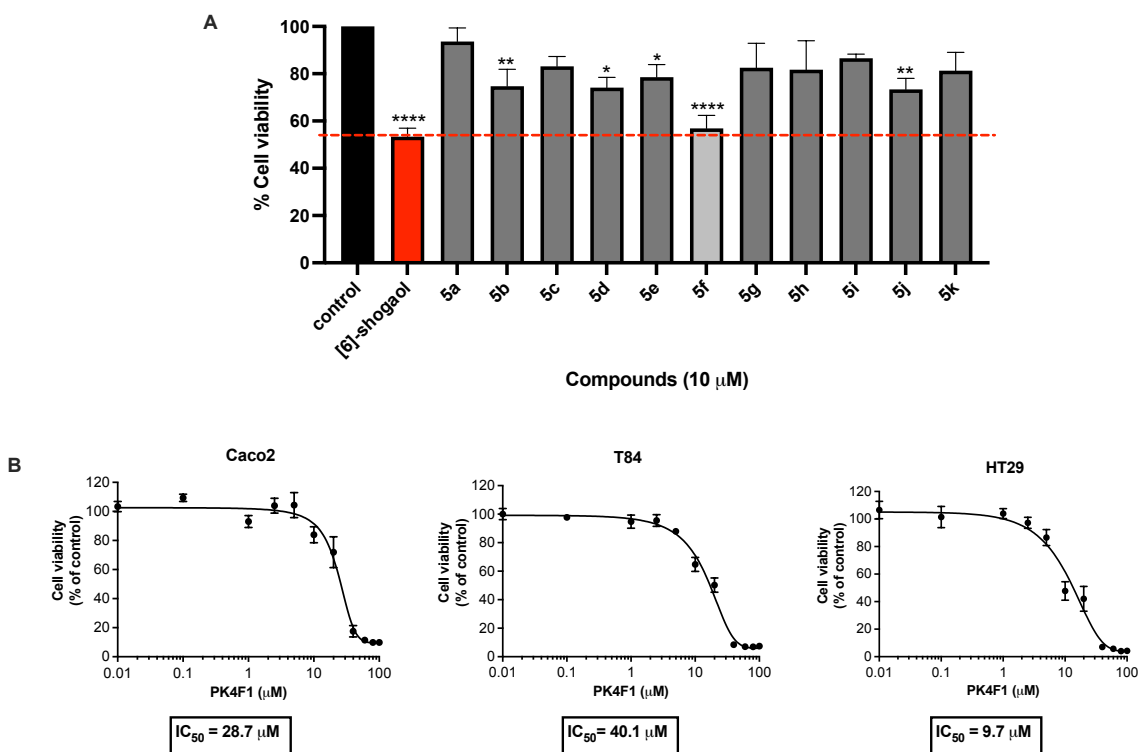**Fig. 1**　Structures of [6]-shogaol and its 11 pyrazole derivatives.

Fig. 2　Effects of pyrazole derivatives of [6]-shogaol on cell viability. (A): Cytotoxic effects of pyrazole derivatives of [6]-shogaol compared with [6]-shogaol in colorectal adenocarcinoma HT29 cells. Cells were treated with each compound at a concentration of 10 μM for 48 h. Cell viability was assessed using the MTT assay and was expressed as a percentage relative to DMSO-treated cells. Data were presented as mean ± SEM of 3–5 independent experiments. * $p < 0.05$ compared with the DMSO-treated cells (B): IC_{50} values of 4F-phenyl pyrazole in three different colorectal cancer cell lines. The IC_{50} values for Caco2, T84, and HT29 cells were 28.1, 40.7, and 9.7 μM, respectively.
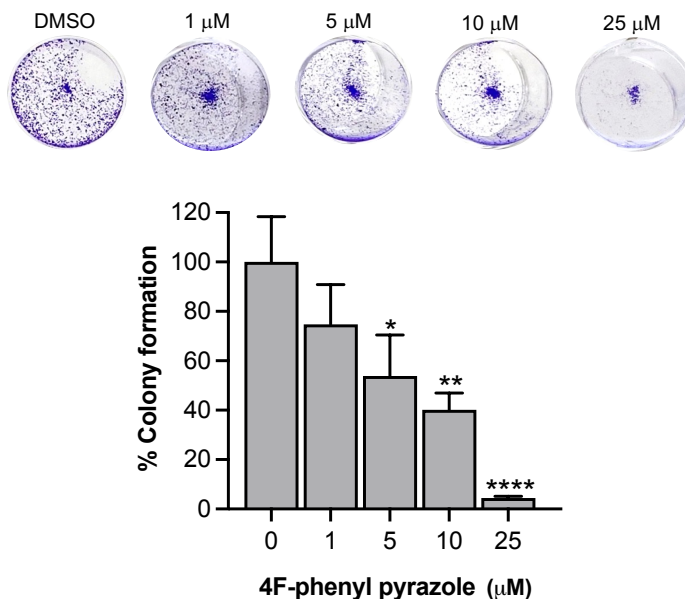
Fig. 3 Cell proliferation of colorectal adenocarcinoma HT29 cells was assessed using a colony formation assay. Cells were treated with 4F-phenyl pyrazole at concentrations ranging from 0 to 25 μM for 7 days. Colonies were visualized by crystal violet staining. The number of colonies significantly decreased in a dose-dependent manner in response to 4F-phenyl pyrazole, indicating reduced cell proliferation. Data were expressed as mean ± SEM. * $p < 0.05$ compared with DMSO-treated cells.
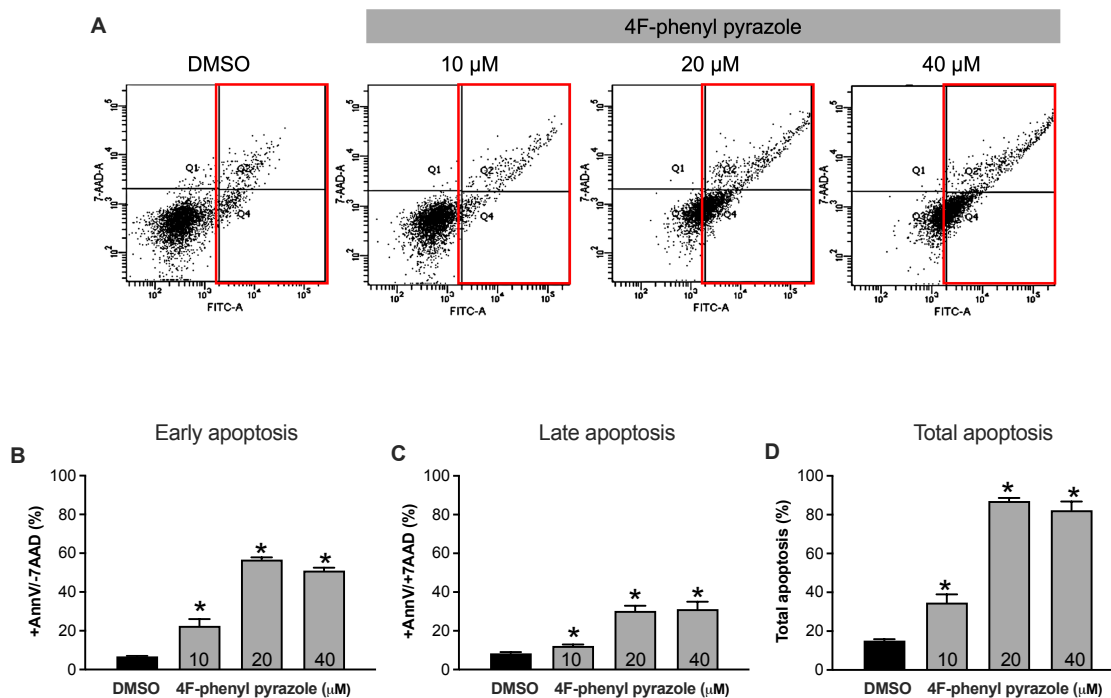

Fig. 4 Flow cytometry analysis of HT29 cells treated with 4F-phenyl pyrazole at concentrations ranging from 10–40 μM for 72 h. (A), Representative flow cytometry plots showing increased annexin V-FITC/7-AAD staining with increasing concentrations of 4F-phenyl pyrazole; (B), percentage of cells in early apoptosis indicated by annexin V-FITC positive and 7-AAD negative staining; (C), percentage of cells in late apoptosis as indicated by double-positive staining for annexin V-FITC and 7-AAD; (D): total percentage of cells undergoing apoptosis. Data were presented as mean percentage ± SEM. * $p < 0.05$ compared with DMSO-treated cells.

through apoptosis activation. In this experiment, HT-29 cells were treated with 4F-phenyl pyrazole for 72 h then stained with FITC-annexinV and 7-AAD. Phosphatidylserine (PS) exposure, which can be detected by FITC-AnnexinV staining, is a key indicator of early apoptosis [18, 19]. The results showed that FITC-annexinV stained cells were largely augmented in cells treated with 10, 20, and 40 µM 4F-phenyl pyrazole compared with the control (DMSO) treatment as shown in Fig. 4A,B. This result indicated that 4F-phenyl pyrazole could induce cells undergoing into early apoptosis within 72 h, and the maximum response reached at 20 µM concentration. In addition, late apoptosis was also evident at the 72-h treatment time point as demonstrated by the increased percentage of 7-AAD positive cells relative to the control (DMSO) group, as shown in Fig. 4A,C. The 7-AAD positive cells indicated the leakage of plasma membrane, which happened in late apoptotic cells. Taken together the aforementioned results, apoptotic cells significantly increased when treated with 4F-phenyl pyrazole at 10, 20, and 40 µM (Fig. 4D). These results suggested that 4F-phenyl pyrazole could induce colorectal adenocarcinoma HT29 into cell death by activating apoptosis.

4F-phenyl pyrazole induced expression of cell death-related proteins

Anoctamin6 (ANO6) is known to be a scramblase protein playing a major role in PS exposure and apoptosis [6]. In the present study, we aimed to examine the expression levels of ANO6 in HT-29 cells subjected to treatment with or without 4F-phenyl pyrazole at 10, 20, and 40 µM for durations of 48 and 72 h. Our findings revealed that after 48 h of treatment, no significant upregulation of ANO6 expression was observed, and a slight increase was detected in cells treated with the concentration of 40 µM. However, after 72 h, the expression of ANO6 was significantly increased, exhibiting a dose-dependent pattern (Fig. 5A,B). Microtubule-associated protein LC3 is a distinct protein widely used for monitoring autophagy. Two isoforms of LC3, LC3-I and LC3-II, are required for cells to undergo autophagy [20]. In this study, we investigated the effects of 4F-phenyl pyrazole on LC3 expression. The result showed that the expression of LC3-I and LC3-II were not changed after 48 h of treatment. However, LC3-I was significantly upregulated after 72 h with similar degree in all treatment concentrations (Fig. 5A,C). Interestingly, LC3-II was largely augmented in a dose-response manner indicating the formation of autophagosome after 72 h treatment (Fig. 5A,D). Collectively, these findings indicated that 4F-phenyl pyrazole could induce cell death in HT-29 cells by upregulating the expression of apoptotic and autophagic markers, which were ANO6 and LC3, respectively.

Effects of 4F-phenyl pyrazole on spheroid formation

Spheroids are an *in vitro* model for cancer study which mimics the conditions of avascular tumors, where there is limited access to oxygen, nutrients, as well as cancer therapeutic drugs. We investigated the HT29 spheroids after treatment with 4F-phenyl pyrazole for 48 h. To assess the effect of 4F-phenyl pyrazole on HT29 spheroids, they were cultured and maintained their uniform and spherical shape with diameter ranging from 200 to 500 µm for 3 days before initiating treatment (day 0) with 4F-phenyl pyrazole (Fig. 6A). Because of the complexity of spheroids compared with monolayer cultures, we started the treatment at 20 µM, which is double the IC$_{50}$ obtained from monolayer studies. We observed concentration-dependent effects after 2 days of 4F-phenyl pyrazole treatment. At 40 µM, the spheroids were unable to maintain a dense structure compared with the DMSO-treated spheroids, which was consistent with a reduction in spheroid solidity (Fig. 6C), indicating a loss of compactness. Lower solidity resulted from a more irregular spheroid boundary was often due to the release of dead cells from the spheroids [21–23]. Although no effect was observed at 20 µM (Fig. 6B,C), we noticed damaged spheroids showing a loss of mass density. Cells on the outer surface of the spheroids were dying and detaching, with increased debris surrounding the spheroids. This coincided with an increase in projected spheroid area (Fig. 6B), which included the area of spheroid formation and loose cell layers [24]. Taken together, these findings indicated that 4F-phenyl pyrazole can induce the loss of the ability to form compact, cohesive spheroids and disrupt the membrane integrity of HT29 spheroids.

DISCUSSION

[6]-shogaol is a natural major compound found in ginger. Various derivatives and biological activities of [6]-shogaol have been demonstrated in many studies. Its anticancer effects can be observed in various cancer cell types such as breast cancer, prostate cancer, colon cancer, and leukemia [11, 12, 14, 17]. The present study showed that 4F-phenyl pyrazole, a pyrazole derivative of [6]-shogaol had a strong cytotoxic effect on colorectal adenocarcinoma HT29 cells with the IC$_{50}$ of 9.7 µM, which was comparable to that of [6]-shogaol (IC$_{50}$ of approximately 9.5 µM) under the same treatment conditions. The colony formation assay showed that 4F-phenyl pyrazole not only killed HT29 cells, but also inhibited cell proliferation and; consequently, the colony formation was reduced, all in a dose-response manner. The results suggested that 4F-phenyl pyrazole was cytotoxic as well as anti-proliferative against colorectal adenocarcinoma HT29 cells. Notably, pyrazole derivatives, including 4F-phenyl pyrazole, have been previously reported to exhibit histone deacetylase
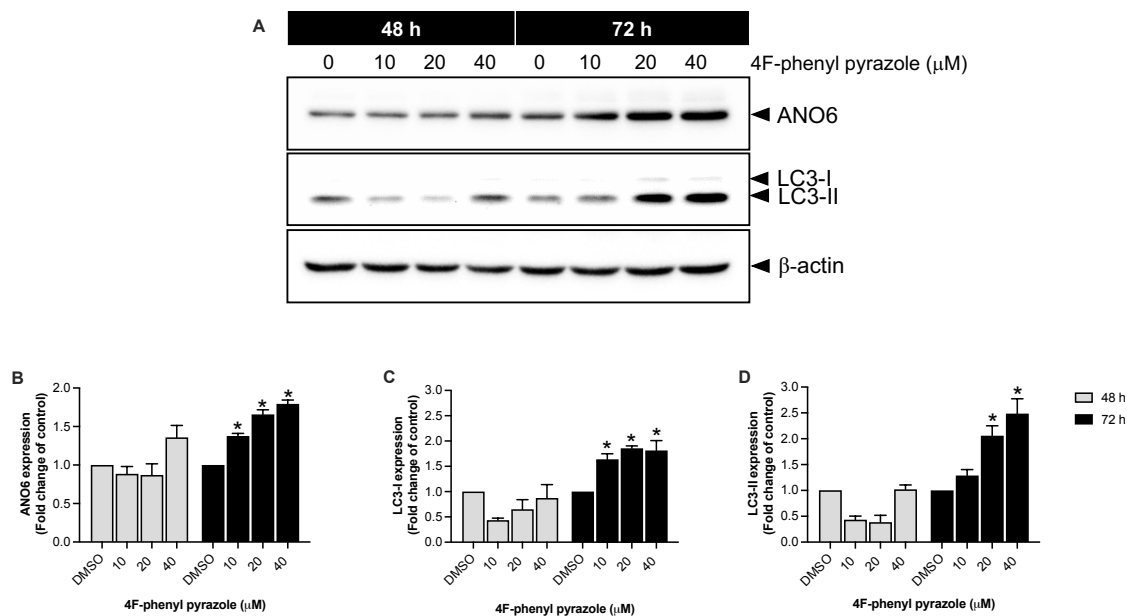
Fig. 5 Western blot analysis of apoptosis and autophagy markers in HT29 cells treated with 4F-phenyl pyrazole. (A), Representative Western blot images showing the expression of anoctamin 6 (apoptosis marker) and LC3-I/II (autophagy markers) in HT29 cells treated with 4F-phenyl pyrazole at a concentration of 10, 20, and 40 μM for 48 and 72 h; (B), quantification of anoctamin 6 expression; (C), quantification of LC3-I expression; (D), quantification of LC3-II expression. Protein expression was quantified using the ChemiDoc™ MP Imaging System. Data were presented as mean ± SEM from three independent experiments. * $p < 0.05$ compared with DMSO-treated cells.

(HDAC) inhibitory activity, ranging from 52% to 85% at 100 μM [16]. HDAC inhibition is a well-established strategy in anti-cancer drug development, as it can lead to the modulation of gene expression, induction of cell cycle arrest, inhibition of cell proliferation, suppression of angiogenesis, and promotion of apoptosis [25]. Therefore, it is plausible that the anti-proliferative effects observed with 4F-phenyl pyrazole treatment could be attributed, at least in part, to its potential HDAC inhibitory activity.

Numerous studies have elucidated the mechanisms underlying the cytotoxic effects of [6]-shogaol. One of the well-established mechanisms is the induction of apoptosis, which has been reported in various cancer cell types, including colon adenocarcinoma, ovarian cancer, breast cancer, and prostate cancer. These studies have revealed that [6]-shogaol can activate different apoptotic pathways in cancer cells, contributing to its anti-cancer properties [11–13, 26]. The present study reveals that 4F-phenyl pyrazole, a synthetic pyrazole derivative of [6]-shogaol, also exhibited cytotoxic effects on colorectal adenocarcinoma HT29 cells, potentially through the induction of apoptosis. Treatment with 4F-phenyl pyrazole resulted in an increased exposure of phosphatidylserine (PS) on the outer leaflet of plasma membrane, as indicated by enhanced annexinV-FITC staining. This PS externalization is a well-known hallmark of early apoptosis,

suggesting that 4F-phenyl pyrazole triggered apoptotic cell death in HT29 cells [27]. PS exposure on the cell surface is a key event in apoptosis and is known to be regulated by anoctamin6 (ANO6), also known as TMEM16F, a member of TMEM16 family. ANO6 functions as both a Ca^{2+}-activated chloride channel and a Ca^{2+}-dependent phospholipid scramblase [6, 7, 28]. The externalization of PS during apoptosis serves as an "eat me" signal, prompting macrophages to engulf and remove apoptotic cells [29]. Therefore, we investigated the effects of 4F-phenyl pyrazole on the ANO6 expression in HT29 cells. Our results demonstrated that ANO6 expression was significantly upregulated after 72 h of treatment with 4F-phenyl pyrazole in a dose-dependent manner. However, while ANO6 expression increased, the magnitude of this increase might not be sufficient to independently trigger cell death.

To further elucidate the cellular mechanisms affected by 4F-phenyl pyrazole, we investigated the expression of microtubule-associated protein LC3, a well-characterized protein associated with autophagy. Autophagy is an intracellular degradation process that eliminates damaged organelles, proteins, and other cellular components [30]. This process involves the formation of autophagosomes, which engulf cellular components targeted for destruction. Subsequently, lysosomes fuse with autophagosomes, leading to the
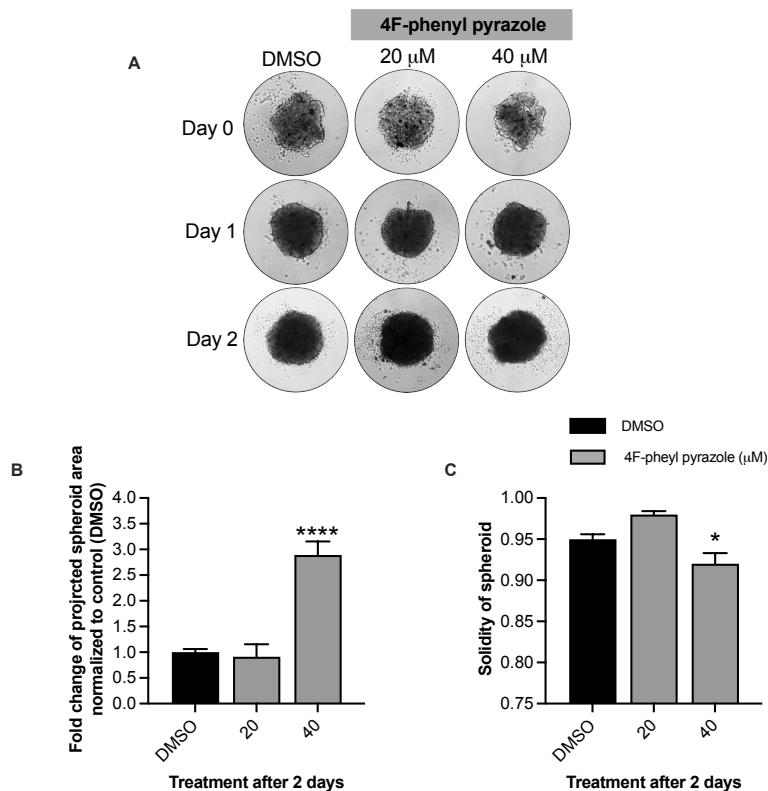
Fig. 6 Effects of 4F-phenyl pyrazole on spheroid formation. (A), Representative brightfield images of HT29 cell spheroids treated with DMSO (control), 20 µM, or 40 µM of 4F-phenyl pyrazole on day 1 and day 2; (B), quantification analysis of projected spheroid area, a measure of spheroid formation area and loose cell layers, presented as fold change normalised to DMSO treated cells. (C), analysis of spheroid solidity, a measure of spheroid density. Data were presented as mean ± SEM from 6–12 independent spheroids for individual treatment groups. * $p < 0.05$ compared with DMSO-treated cells, **** $p < 0.0001$ compared with DMSO-treated cells.

degradation of the engulfed content. The formation of autophagosomes requires two forms of LC3 protein: LC3-I and LC3-II. LC3-I is cytosolic, while LC3-II is formed by the conjugation of LC3-I with phosphatidylethanolamine (PE). The conjugation facilitates autophagosome elongation and formation. Although autophagy is generally considered a pro-survival mechanism, it has also been described as a control mechanism for suppressing cancer formation [31–33]. Previous studies have shown that [6]-shogaol can induce autophagic cell death in colorectal adenocarcinoma HT29 cells [9]. Similarly, [6]-shogaol has been reported to inhibit cell proliferation by inducing autophagy in human non-small cell lung cancer A549 cells and breast cancer cells, both in monolayer and cancer stem cell-like spheroid cultures [14, 34]. In the present study, we investigated whether 4F-phenyl pyrazole, a pyrazole derivative of [6]-shogaol, affecting autophagic processes in HT29 colorectal adenocarcinoma cells. Our results demonstrated that treatment with 4F-phenyl pyrazole increased the expression of cytosolic form of

LC3 (LC3-I) in HT29 cells. However, this increase in LC3-I expression did not show a dose-dependent relationship with 4F-phenyl pyrazole concentration. Interestingly, the expression of LC3-II, the conjugated form indicating autophagosome formation, increased significantly in a dose-dependent manner. Collectively, these findings suggested that 4F-phenyl pyrazole might potentially induce cell death by activating both apoptosis and autophagy through the increased expression of key proteins involved in these processes, namely anoctamin6 and LC3, respectively.

Our investigation extended to examining the effects of 4F-phenyl pyrazole on spheroid formation, an important aspect of cancer cell behavior. Spheroids serve as a three-dimensional (3D) *in vitro* model, closely mimicking tumor microenvironments, particularly in terms of heterogeneous access to nutrients, oxygen, and chemotherapeutic agents [35, 36]. Compared with the inner regions, the outer layers of spheroids are typically more exposed to treatment factors. At 40 µM, 4F-phenyl pyrazole treatment resulted

in a substantial increase in projected spheroid area which served as a measure for spheroid formation and loose cell-cell contacts [24]. The loss of spheroid integrity was reflected in cells spreading out from the compact structure, compromised cell-cell adhesion, or perhaps increased cell damage, with dead cells detaching from the outer layers and increased debris surrounding the spheroids after exposure to toxic substances [21, 24]. Our results demonstrated that treatment with 4F-phenyl pyrazole led to cell dispersion from spheroids, which was observed as increased cell-covered and projected spheroid area. Moreover, looser compactness of spheroids and more dispersed cells surrounding spheroids were likely due to the ability of 4F-phenyl pyrazole to enhance cell death, as evidenced by the detachment of dead cells from the outer layer of spheroids [36–40]. The observation correlated with clearly attenuated proliferation and induced both apoptosis and autophagy in HT29 cells after 4F-phenyl pyrazole treatment. Collectively, our results showed that spheroids treated with 4F-phenyl pyrazole lost its compactness and regularity of the surface. Tightly packed spheroids with uniform surfaces are characteristic features of cancer cell aggregates, often associated with tumorigenic properties [36, 37, 40]. The ability of 4F-phenyl pyrazole to compromise the structural integrity of spheroids might have significant implications for its potential as an anti-cancer agent. By disrupting the capacity of colorectal adenocarcinoma HT29 cells to form and maintain these three-dimensional structures, the compound could potentially inhibit tumor formation.

Our study provided insights into the anticancer potential of 4F-phenyl pyrazole, a derivative of the well-studied [6]-shogaol. While both compounds demonstrated similar effects on cell viability, our investigation revealed that 4F-phenyl pyrazole influenced specific cancer-related pathways, particularly the upregulation of ANO6 expression associated with enhanced apoptosis. This finding suggested a potentially unique mechanism of action for 4F-phenyl pyrazole. However, it is crucial to note that we did not directly compare the effects of [6]-shogaol on ANO6 expression in this study, highlighting an important area for future researches. Furthermore, although the cell viability results were comparable, 4F-phenyl pyrazole might possess distinct pharmacological properties from [6]-shogaol. These potential differences in aspects such as bioavailability, metabolic stability, and toxicity profiles necessitate further investigation.

CONCLUSION

In conclusion, our study demonstrated that 4F-phenyl pyrazole, a pyrazole derivative of [6]-shogaol, exhibits promising potential as an anti-cancer compound. 4F-phenyl pyrazole exerted cytotoxic effects on colorectal adenocarcinoma HT29 cells and inhibited spheroid formation. The compound's cytotoxicity appeared to be mediated through the upregulation of ANO6 and LC3 proteins, key players in apoptosis and autophagy pathways, respectively. However, the precise molecular mechanisms underlying the increased expression of ANO6 and LC3, as well as the disruption of spheroid formation, remain to be fully elucidated. Further study to unravel these mechanisms would provide valuable insights into the compound's mode of action and potentially reveal new therapeutic targets for colorectal cancer treatment.

REFERENCES

1. Xi Y, Xu P (2021) Global colorectal cancer burden in 2020 and projections to 2040. *Transl Oncol* **14**, 101174.
2. Keum N, Giovannucci E (2019) Global burden of colorectal cancer: emerging trends, risk factors and prevention strategies. *Nat Rev Gastroenterol Hepatol* **16**, 713–732.
3. Dekker E, Tanis PJ, Vleugels JLA, Kasi PM, Wallace MB (2019) Colorectal cancer. *Lancet* **394**, 1467–1480.
4. Sjöström J, Bergh J (2001) How apoptosis is regulated, and what goes wrong in cancer. *BMJ* **322**, 1538–1539.
5. Lossi L (2022) The concept of intrinsic versus extrinsic apoptosis. *Biochem J* **479**, 357–384.
6. Suzuki J, Umeda M, Sims PJ, Nagata S (2010) Calcium-dependent phospholipid scrambling by TMEM16F. *Nature* **468**, 834–838.
7. Kunzelmann K, Ousingsawat J, Benedetto R, Cabrita I, Schreiber R (2019) Contribution of anoctamins to cell survival and cell death. *Cancers* **11**, 382.
8. Mahgoub E, Taneera J, Sulaiman N, Saber-Ayad M (2022) The role of autophagy in colorectal cancer: Impact on pathogenesis and implications in therapy. *Front Med* **9**, 959348.
9. Du Y-X, Mamun AA, Lyu A-P, Zhang H-J (2023) Natural compounds targeting the autophagy pathway in the treatment of colorectal cancer. *Int J Mol Sci* **24**.
10. Desantis V, Saltarella I, Lamanuzzi A, Mariggiò MA, Racanelli V, Vacca A, Frassanito MA (2018) Autophagy: A new mechanism of prosurvival and drug resistance in multiple myeloma. *Transl Oncol* **11**, 1350–1357.
11. Li T-Y, Chiang B-H (2017) 6-shogaol induces autophagic cell death then triggered apoptosis in colorectal adenocarcinoma HT-29 cells. *Biomed Pharmacother* **93**, 208–217.
12. Saha A, Blando J, Silver E, Beltran L, Sessler J, DiGiovanni J (2014) 6-Shogaol from dried ginger inhibits growth of prostate cancer cells both *in vitro* and *in vivo* through inhibition of STAT3 and NF-κB signaling. *Cancer Prev Res* **7**, 627–638.
13. Kim MO, Lee M-H, Oi N, Kim S-H, Bae KB, Huang Z, Kim DJ, Reddy K, et al (2014) [6]-shogaol inhibits growth and induces apoptosis of non-small cell lung cancer cells by directly regulating Akt1/2. *Carcinogenesis* **35**, 683–691.
14. Ray A, Vasudevan S, Sengupta S (2015) 6-Shogaol inhibits breast cancer cells and stem cell-like spheroids by

modulation of notch signaling pathway and induction of autophagic cell death. *PLoS One* **10**, e0137614.

15. Phaosiri C, Yenjai C, Senawong T, Senawong G, Saenglee S, Somsakeesit L, Kumboonma P (2022) Histone deacetylase inhibitory activity and antiproliferative potential of new [6]-Shogaol derivatives. *Molecules* **27**.

16. Kumboonma P, Senawong T, Saenglee S, Yenjai C, Phaosiri C (2017) Identification of phenolic compounds from *Zingiber offinale* and their derivatives as histone deacetylase inhibitors and antioxidants. *Med Chem Res* **26**, 650–661.

17. Liu Q, Peng Y-B, Zhou P, Qi L-W, Zhang M, Gao N, Liu E-H, Li Ping (2013) 6-Shogaol induces apoptosis in human leukemia cells through a process involving caspase-mediated cleavage of eIF2α. *Mol Cancer* **12**, 135.

18. Nagata S, Suzuki J, Segawa K, Fujii T (2016) Exposure of phosphatidylserine on the cell surface. *Cell Death Differ* **23**, 952–961.

19. Bevers EM, Williamson PL (2016) Getting to the outer leaflet: Physiology of phosphatidylserine exposure at the plasma membrane. *Physiol Rev* **96**, 605–645.

20. Mizushima N, Yoshimori T (2007) How to interpret LC3 immunoblotting. *Autophagy* **3**, 542–545.

21. Hornung A, Poettler M, Friedrich RP, Weigel B, Duerr S, Zaloga J, Cicha I, Alexiou C, et al (2016) Toxicity of mitoxantrone-loaded superparamagnetic iron oxide nanoparticles in a HT-29 tumour spheroid model. *Anticancer Res* **36**, 3093–3101.

22. Simelane NWN, Abrahamse H (2024) Actively targeted photodynamic therapy in multicellular colorectal cancer spheroids via functionalised gold nanoparticles. *Artif Cells Nanomed Biotechnol* **52**, 309–320.

23. Štampar M, Breznik B, Filipič M, Žegura B (2020) Characterization of *in vitro* 3D cell model developed from human hepatocellular carcinoma (HepG2) cell line. *Cells* **9**, 2557.

24. Stadler M, Scherzer M, Walter S, Holzner S, Pudelko K, Riedl A, Unger C, Kramer N, et al (2018) Exclusion from spheroid formation identifies loss of essential cell-cell adhesion molecules in colon cancer cells. *Sci Rep* **8**, 1151x.

25. Hontecillas-Prieto L, Flores-Campos R, Silver A, de Álava E, Hajji N, García-Domínguez DJ (2020) Synergistic enhancement of cancer therapy using HDAC inhibitors: Opportunity for clinical trials. *Front Genet* **11**, 578011.

26. Kim TW, Lee HG (2023) 6-Shogaol overcomes gefitinib resistance via ER stress in ovarian cancer cells. *Int J Mol Sci* **24**, 2639.

27. Frasch SC, Henson PM, Kailey JM, Richter DA, Janes MS, Fadok VA, Bratton DL (2000) Regulation of phospholipid scramblase activity during apoptosis and cell activation by protein kinase Cdelta. *J Biol Chem* **275**, 23065–23073.

28. Kunzelmann K, Nilius B, Owsianik G, Schreiber R, Ousingsawat J, Sirianant L, Wanitchakool P, Bevers EM, et al (2014) Molecular functions of anoctamin 6 (TMEM16F): a chloride channel, cation channel, or phospholipid scramblase? *Pflugers Arch* **466**, 407–414.

29. Wu N, Veillette A (2023) Lipid scrambling in immunology: why it is important. *Cell Mol Immunol* **20**, 1081–1083.

30. Levine B, Klionsky DJ (2004) Development by self-digestion: molecular mechanisms and biological functions of autophagy. *Dev Cell* **6**, 463–477.

31. Tanida I, Ueno T, Kominami E (2008) LC3 and Autophagy. *Methods Mol Biol* **445**, 77–88.

32. Li X, He S, Ma B (2020) Autophagy and autophagy-related proteins in cancer. *Mol Cancer* **19**, 12.

33. Yun CW, Lee SH (2018) The roles of autophagy in cancer. *Int J Mol Sci* **19**, 3466.

34. Hung J-Y, Hsu Y-L, Li C-T, Ko Y-C, Ni W-C, Huang M-S, Kuo P-L (2009) 6-Shogaol, an active constituent of dietary ginger, induces autophagy by inhibiting the AKT/mTOR pathway in human non-small cell lung cancer A549 cells. *J Agric Food Chem* **57**, 9809–9816.

35. Palliyage GH, Ghosh R, Rojanasakul Y (2020) Cancer chemoresistance and therapeutic strategies targeting tumor microenvironment. *ScienceAsia* **46**, 639–649.

36. Weiswald L-B, Bellet D, Dangles-Marie V (2015) Spherical cancer models in tumor biology. *Neoplasia* **17**, 1–15.

37. Białkowska K, Komorowski P, Bryszewska M, Miłowska K (2020) Spheroids as a type of three-dimensional cell cultures-examples of methods of preparation and the most important application. *Int J Mol Sci* **21**, 6225.

38. Costa EC, Moreira AF, de Melo-Diogo D, Gaspar VM, Carvalho MP, Correia IJ (2016) 3D tumor spheroids: an overview on the tools and techniques used for their analysis. *Biotechnol Adv* **34**, 1427–1441.

39. Amaral RLF, Miranda M, Marcato PD, Swiech K (2017) Comparative analysis of 3D bladder tumor spheroids obtained by forced floating and hanging drop methods for drug screening. *Front Physiol* **8**, 605.

40. Amaral RLF, Miranda M, Marcato PD, Swiech K (2016) Comparative analysis of tumor spheroid generation techniques for differential *in vitro* drug toxicity. *Oncotarget* **7**, 16948–16961.